Human Cadaver and Hybrid III Responses to Axial Impacts of the Femur

Richard M. Morgan
Rolf H. Eppinger
Jeffrey H. Marcus
U. S. DOT/NHTSA

Hunter Nichols
Consis Corp.
U. S.

ABSTRACT This study examined the responses of 126 human cadaver and 222 Hybrid III dummy femurs undergoing dynamic axial impact.

First, for human cadaver leg impacts, applied femur force alone was shown to do a good job of separating injury from non-injury. The combination of applied femur force and femur force rise time also was investigated.

Second, 191 Hybrid III femur responses in vehicle collisions were explored. For belt and air bag restrained occupants, it was found that the Hybrid III femur data points fall in the non-injury region for the human cadaver leg. The few data points which fall in the injury region are from vehicle collisions in which there was substantial intrusion of the firewall and instrument panel.

For seven separate laboratory test conditions of human cadaver patella-femur-pelvis impact, femur-force-versus-time corridors were constructed for mass scaled cadavers. The Hybrid III response was overlaid on the cadaver corridor to show the extent to which the Hybrid III mimics the human cadaver. Impulse-versus-time cadaver corridors and Hybrid III impulse-versus-time overlays were also constructed.

In a final step, the Hybrid III femur response was examined relative to human cadaver injury. In six of the seven laboratory test conditions, the Hybrid III predicted injury for the injured cadavers and non-injury for the non-injured cadavers. One set of sled experiments — in which the cadaver femur and the Hybrid III femur may not respond the same — was discussed.

INTRODUCTION About patella-femur-pelvis injury, researchers [1, 2, 3, 4, 5, 6, 7, 8][1] have suggested that a reasonable femur injury criterion to prevent bone damage is to limit the axial compressive load.

Several investigators of impacts to the lower extremities of unembalmed human cadavers said that force alone may not be sufficient to separate injury from non-injury. Leung et al. [8] found the tolerance to fracture to depend also on the cadaverous subject's bone condition.

Cooke and Nagel [3] said the severity of trauma produced depended on both the peak forces generated and the impact energy absorbed. Melvin et al. [5] also saw — for distal fractures of the femur and patella — the peak axial force is not an adequate indicator of potential fracture and the kinetic energy level associated with the impact must also be considered. They saw their fractures typically exhibited a single "sharp load peak" as shown in Figure 1 and non-fractures exhibited a "double peaked" wave form.

Injuries to the patella-femur-pelvis — and to the lower extremities

---

[1]Numbers in brackets designate references at end of paper.

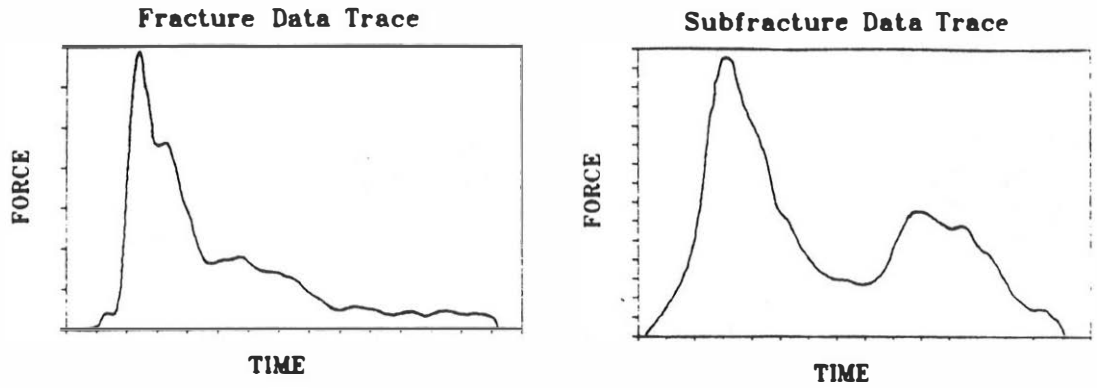

Fig. 1 - Shape of applied femur force reported in Reference 5

in general — are seldom fatal, but often require longer hospitalization and more lost working days than injuries (of equal AIS numbers) to other parts of the body. [9, 10] One investigator looking at hospitalization and rates of inpatient/outpatient health services noted "Recent studies have shown, however, that lower extremity injuries represent the second most important source of disability among individuals who survive traumatic injury; this fact has largely gone unrecognized." [11] An examination of NASS data for 1982 through 1985 also found lower extremity injuries to be the second most important source of impairment. [12]

NASS DATA FILES The 1982-1986 National Accident Sampling System (NASS) files examined in this section satisfied the following criteria: (1) frontal impacts, (2) the vehicle was a passenger car or light truck or van, (3) the vehicle was not in a rollover, (4) either a driver or a right front seat passenger, (5) age of the injured person was 16 years or older, and (6) the occupant was not ejected. The injury counts are weighted by a national expansion factor to make the NASS files representative of the population of accidents which occur in the United States. In examining the knee-thigh-hip injuries, be aware of how injuries were coded in the 1982-1986 NASS files. A maximum of six injuries may be coded for a single "NASS occupant," with each injury coded according to AIS standard conventions. If an occupant had multiple injuries, the more severe injuries were coded first. Since the highest AIS value available for the entire lower extremities is a four, the NASS coders may not have got to the lower extremities (body region) for an occupant with many injuries.

Figure 2 shows the distribution of injuries by body region for belted occupants. The solid bars are the percentage of AIS counts for AIS greater than or equal to two. All the solid bars should sum to 100 percent of the total AIS >= 2 injuries for belted occupants. The crosshatched bars are the percentage of harm [13, 14] corresponding to the AIS >= 2 values. The knee-thigh-hip injuries are about 12 percent of the total AIS >= 2 count for belted occupants.

Figure 3 shows the distribution of injuries by body region for non-belted occupants. Again, the knee-thigh-hip region are about 13 percent of the total AIS >=2 count for non-belted occupants.

Figure 4 breaks down the knee-thigh-hip bar of Figure 2. For belted occupants, the knee accounts for about 61 percent of the knee-thigh-hip AIS >= 2 count. The thigh accounts for about 47 percent of the harm (AIS >= 2). Figure 4 also breaks down the knee-thigh-hip bar of Figure 3. For non-belted occupants, the knee accounts for about 44 percent of the knee-thigh-hip AIS >= 2 count. The thigh accounts for about 42 percent of the harm.

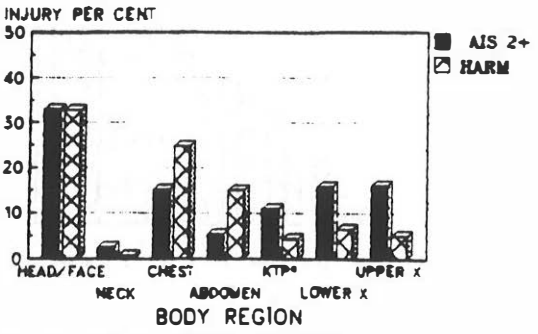

Fig. 2 - Distribution of injuries to belted occupants

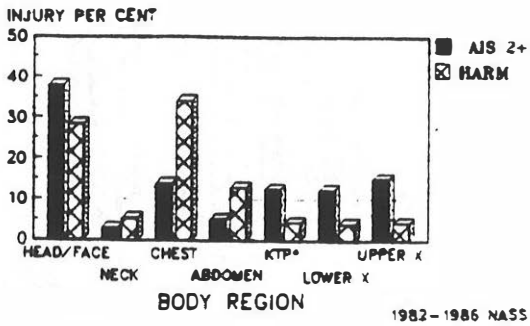

Fig. 3 - Distribution of injuries to non-belted occupants

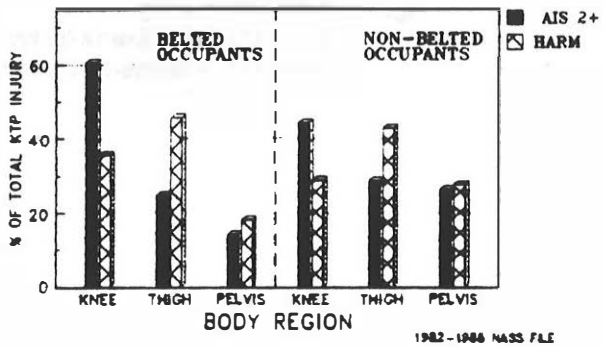

Fig. 4 - Distribution of knee-thigh-pelvis injuries

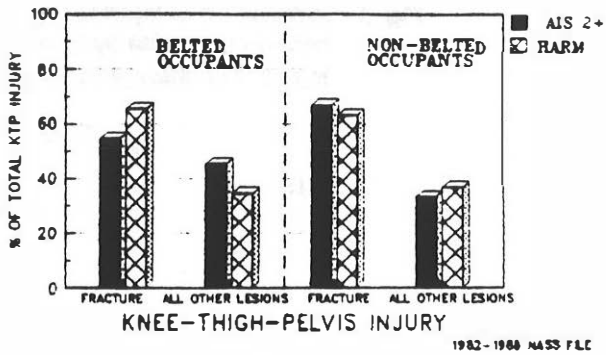

Fig. 5 - Distribution of fractures and other lesions

Later in this paper, the analysis of injuries from laboratory impacts of human cadavers will be presented. Most of the laboratory based injuries are bone fractures. The question naturally arises, "Are fractures a significant portion of NASS knee-thigh-hip lesions ?" Figure 5, for belted and non-belted occupants, shows fractures are the major part of the AIS >= 2 count and also the harm.

Figures 6 and 7 show the distribution of knee-thigh-hip injuries by change-in-velocity for belted and non-belted occupant respectively. Only about 50 percent or less of the NASS cases have the information necessary for the calculation of change-of-velocity. Because of the requirement the NASS case have a calculated change-of-velocity, the number of usable crashes goes down. We have previously pointed out that — for severely injured occupants — the NASS coder may not have got to the lower extremity injuries. Because of these reasons, Figure 6 represents only 24 occupants for "other injuries" (unweighted NASS files) and should be interpreted with caution.

LABORATORY DATA Hybrid III dummies were tested in pendulum, sled, and vehicle tests. The direction of the impact loading of the Hybrid III was frontally into the patella-femur-pelvis complex through the patella. Since 1982, 101 Hybrid III dummies underwent testing in twenty-two different vehicle makes and models. Some vehicles were crashed into a rigid barrier at speeds ranging from 41- to 57-kph while others were vehicle-to-vehicle full-frontal or offset impacts at 57- to 114-kph closing velocity.

The remaining tests selected for this study were frontal impacts to the patella of unembalmed human cadavers. These tests were from four agency-sponsored studies [15, 16, 17, 18, 19] and from two studies in the literature. [8, 20] The impacting device was either a pendulum or sled. (See the original references and Reference 21 for details.)

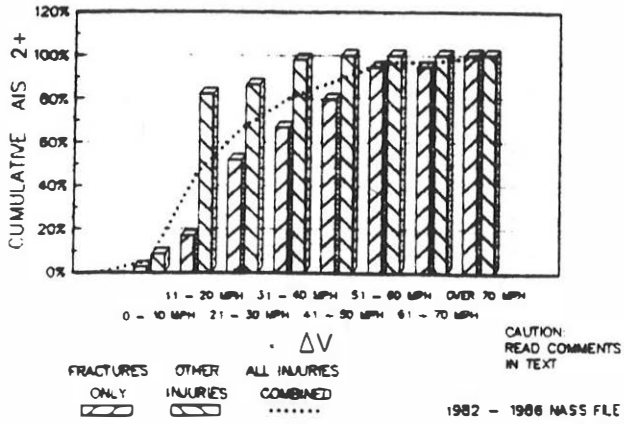

Fig. 6 - Distribution of injuries to belted occupants by type injury and change-in-velocity

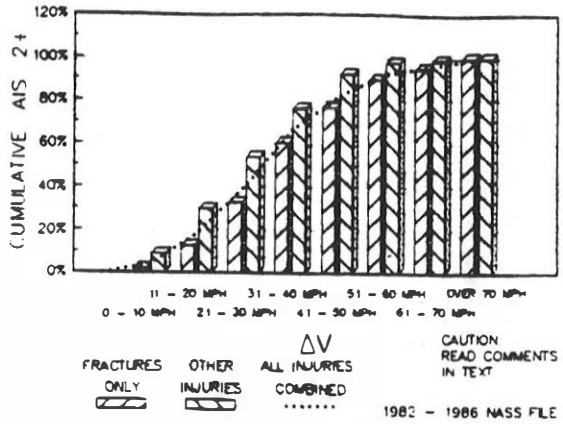

Fig. 7 - Distribution of injuries to non-belted occupants by type injury and change-in-velocity

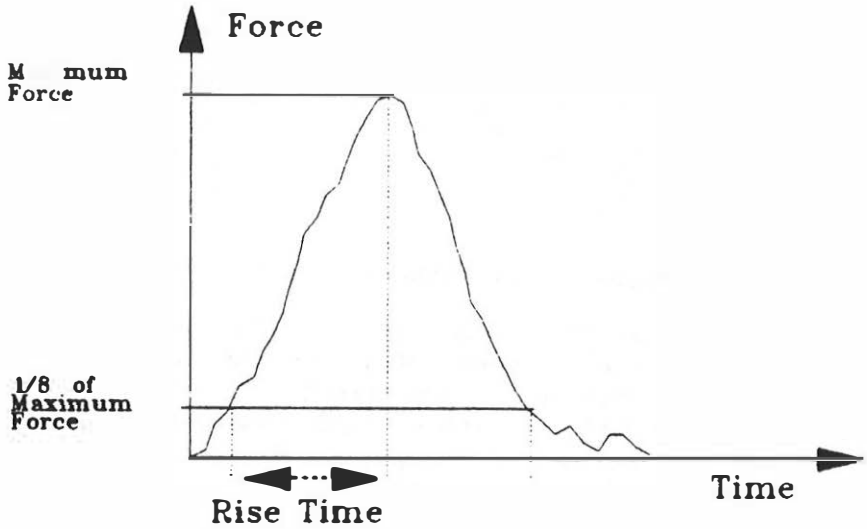

Fig. 8 - Illustration of rise time

The SAE recommended filter for femur force is Class 600. To the eyes of at least one of the authors, many of the SAE Class 600 femur force signals appeared as "spiky traces" and looked like the "raw traces" (the SAE Class 1000 traces). In this paper, all femur force data was processed with a Class 180 filter.

The rise time — see Figure 8 — is defined as the difference of the time of maximum femur force and the time at 1/8th of the peak force.

The impulse is the integration of the femur force. (The integration begins at the time of zero force and not the time at 1/8th of the peak force.)

INJURY INDEX Some short mention should be made of a previous paper, [21] though space limitations forbid any extended discussion. Based on 112 patella-femur-pelvis impact experiments, applied femur force alone did a reasonably good job of separating injury/non-injury as shown in Figure 9. There is a region of lower values of force for which there are no patella-femur-pelvis injuries. Next, there is a transition region in which both injuries and non-injuries are observed. Lastly, non-injuries disappear for the higher force values. Some 54% (60/112) of the data

points fall in the transition region of Figure 9.

A probability of injury — founded on applied femur force as the lone independent variable — was developed using a Weibull distribution and the Maximum Likelihood Method and is presented in Figure 10. [22, 23] A force value of 10 kN (2250 pounds) is at the 35 % level of injury risk.

A discrimination capability between injury/non-injuries was established using a bivariant model with F_{max} and T_{rise} as the independent variables as shown in Figure 11. In particular, the 21% probability line of injury goes up to about 12 kN for T_{rise} <= 10 msec. After 10 msec, where does the 21 % probability line go ? Since there are no injuries after 10 msec for this data set, the non-injury region was arbitrarily capped by a horizontal femur force line at F_{max} = 12 kN. No injury was seen below 7.0 kN.

Figure 12 shows injury versus the best — in the Discriminant Analysis sense [24,25] — linear combination of maximum applied femur force and rise time for the data subsample where $T_{Rise\ Time}$ < = 10 msec. The transition region — i. e., the overlap where both injury and non-injury happen — covers only 41% (46/112) of all the data points.

The patella-femur-pelvis injuries of the human cadavers are described in Reference 21. Most are fractures although there are lacerations. Our data sample does not possess a solitary femoral shaft fracture without injury to the patella or femoral condyles, which solitary type of injury is reported in real world collisions. [26] It appears our data sample is more representative of the kind of injury which occurs when the knee impacts stiff, unyielding structures.

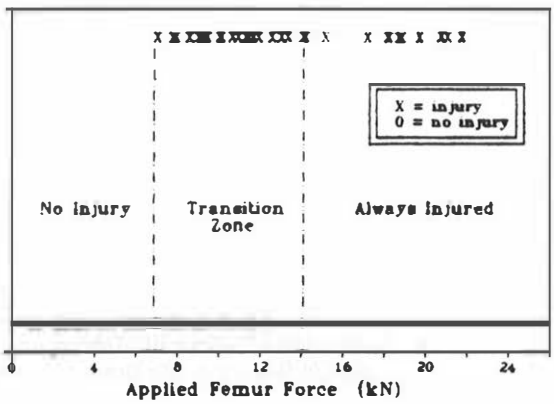

Fig. 9 - Injury/non-injury vs applied femur force

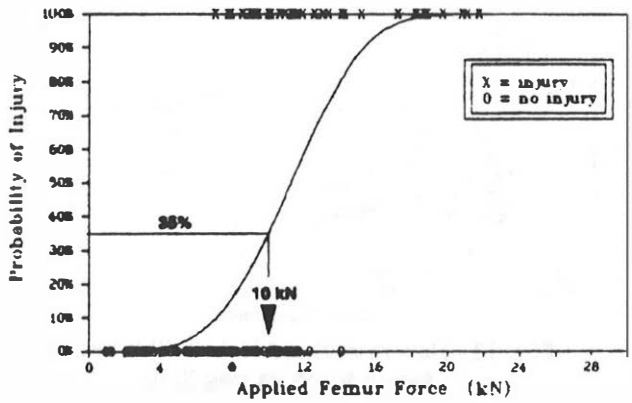

Fig. 10 - Probability of injury vs applied femur force

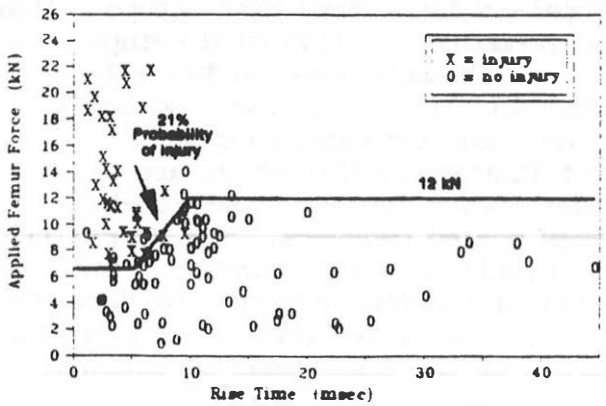

Fig. 11 - Maximum applied femur force vs rise time

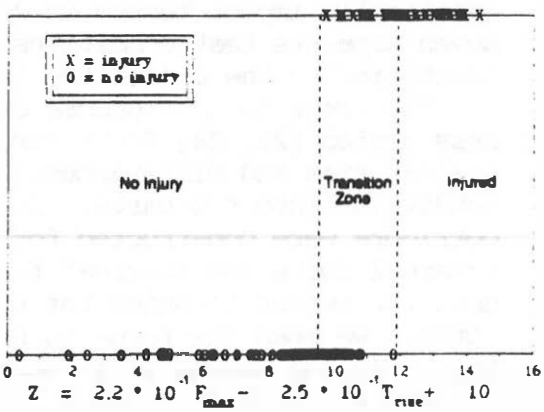

Fig. 12 - Injury/non-injury vs applied femur force and rise time

HYBRID III TESTS A summary of the vehicles crashed, the test condition, and the Hybrid III response is in Table 1. Table 2 lists the Hybrid III response for the sled and pendulum tests.

It has been mentioned before that maximum femoral force and femoral force rise time are parameters of interest. A plot of the Hybrid III maximum internal force versus rise time is exhibited in Figure 13 for the vehicle-to-vehicle and vehicle-to-barrier crash tests in which the Hybrid III is non-restrained. On Figure 13, one can overlay the curve — discussed in the previous section — which roughly separates patella-femur-pelvis injury from non-injury for the human cadaver. This figure shows that the most of the Hybrid III data points fall in the non-injury region even though the dummies were unrestrained.

A plot of the Hybrid III maximum internal force versus rise time is exhibited in Figure 14 for the vehicle-to-vehicle and vehicle-to-barrier crash tests in which the Hybrid III is restrained. There are two types of belt restraints and an air bag indicated in Figure 14. The average internal femur force for the 2-point restrained occupants may be slightly higher than for the 3-point restrained occupants; but in general, there is not a clear separation of the femur loads for the two restraint types.

Almost all the restrained Hybrid III data points fall in the non-injury region for the human cadaver leg. The four data points which fall in the injury region are from vehicle collisions in which there was substantial intrusion of the firewall and instrument panel.

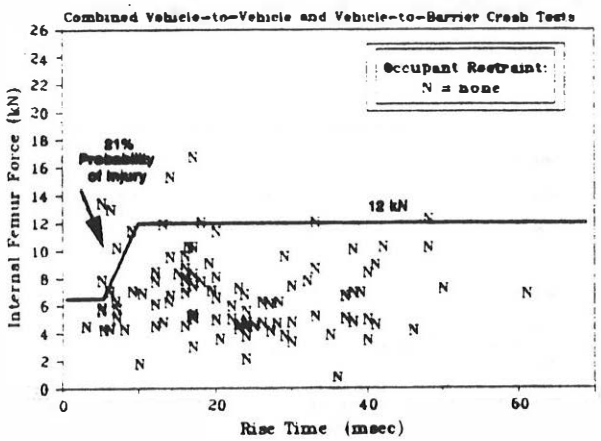

Fig. 13 - Non-restrained Hybrid III internal femur force vs rise time

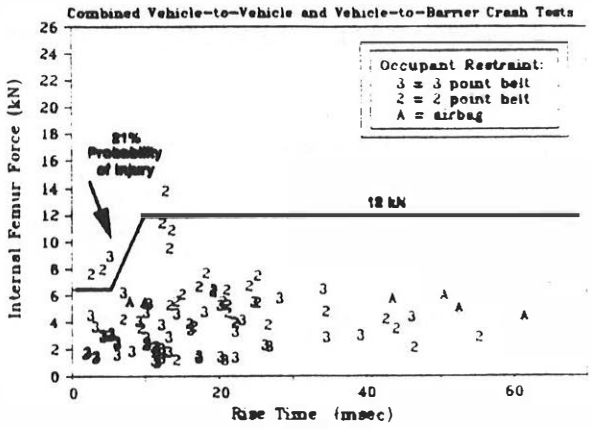

Fig. 14 - Restrained Hybrid III internal femur force vs rise time

HUMANLIKE RESPONSE A number of human cadavers and Hybrid III dummies were identically impact tested in seven separate laboratory test setups. These seven separate test conditions — two pendulum and five sled setups — are identified by the use of the integers one through seven in Table 2.

The femur force response of the Hybrid III will be compared to the mass scaled [27, 28] femur force of the human cadavers to show similarities and differences. Each of Figures 15 through 21 are subdivided into two parts. In part one, femur-force-versus-rise-time corridors were constructed for the mass scaled cadavers. The Hybrid III external force and internal force are overlaid on the cadaver corridor to show the extent to which the Hybrid III mimics the cadaver. By "external force," we mean the force is measured outside of the cadaver or Hybrid III body. In the second part, the integrals of the human cadaver external force are compared to the integral of the Hybrid III external force and internal force. So, the impulse of the human cadavers is compared to the impulse of the Hybrid III for external force and internal force.

These plots are assumed to be one measure of how humanlike the Hybrid III is. One sweeping position to take — based on Figures 15 through 21 — is that the Hybrid III has a higher applied force than the cadavers for the pendulum tests, but the Hybrid III looks like the cadavers for the sled tests.

In looking at Figures 15 and 16, what can we conclude ? For the pendulum impacts, the Hybrid III external and internal force is greater than the mass-scaled human cadaver external force.

For the sled tests in Figures 17 through 20, the Hybrid III external force is close to the human cadaver corridor but slightly high. The Hybrid III internal force is close to but slightly lower than the human cadaver external force levels.

A noteworthy exception was the second (Figure 21) of the two Wayne State University 2-point belt restrained sled tests. In the way of particulars, both Wayne State sled test situations are for a delta-v of 48-kph. The first test condition (Figure 20) has a peak sled acceleration of 22 g's while the second (Figure 21) has 35 g's. The cadaver corridors are similar for both test conditions. The Hybrid III in the first case is close to the mass scaled cadaver corridors as mentioned in the preceding paragraph. For the second case, the Hybrid III external force is much higher than the cadaver external force corridor and the Hybrid III impulse is also higher than the cadaver impulse corridor.

For the seven laboratory test conditions, to what degree does the Hybrid III predict non-injury when the cadavers (knee-thigh-hip body region) were not injured and predict injury when the cadavers (knee-thigh-hip body region) were injured ? Figure 22 displays all the cadaver data and the Hybrid III responses in the seven test conditions (designated 1 through 7 as in Table 2). The vertical axis is the external femur force and the horizontal axis is the rise time linked with the external femur force. In six out of the seven test conditions, the Hybrid III predicts no injury when there were no cadaver lesions and predicts injury when there were cadaver lesions. In Figure 22, the symbol "6" is the Hybrid III response in the second 2-point belt restrained Wayne State University sled test. Although the cadaver had no lesions in the second Wayne State sled test, the Hybrid III predicts occurrence of injury.

Figure 23 is similar to Figure 22, but the Hybrid III internal femur force is used in place of the Hybrid III's external femur force. The results are the same in that the Hybrid III again predicts correctly in six out of the seven laboratory test conditions.

FIG. 15 - CALSPAN PADDED PENDULUM 27 KPH APPLIED FEMUR FORCE AND IMPULSE CORRIDORS

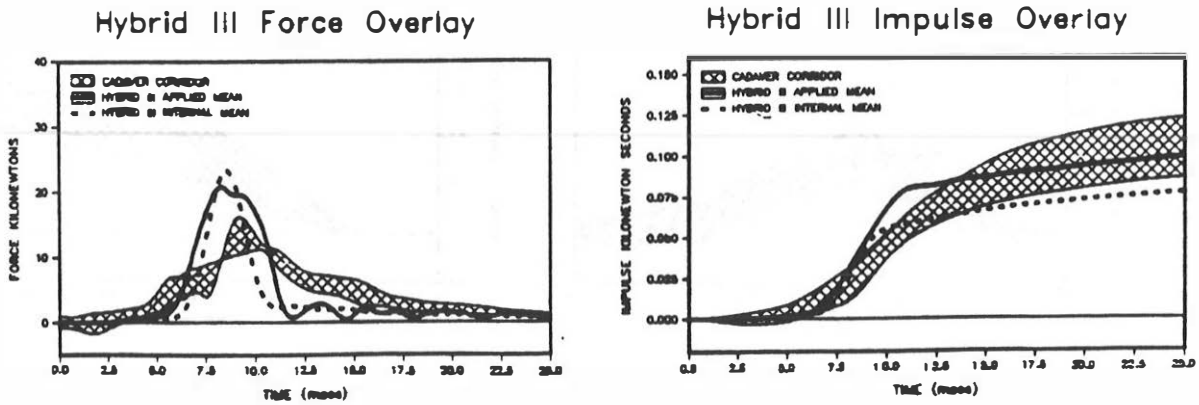

FIG. 16 - CALSPAN PENDULUM (NO PAD) 27 KPH APPLIED FEMUR FORCE AND IMPULSE CORRIDORS

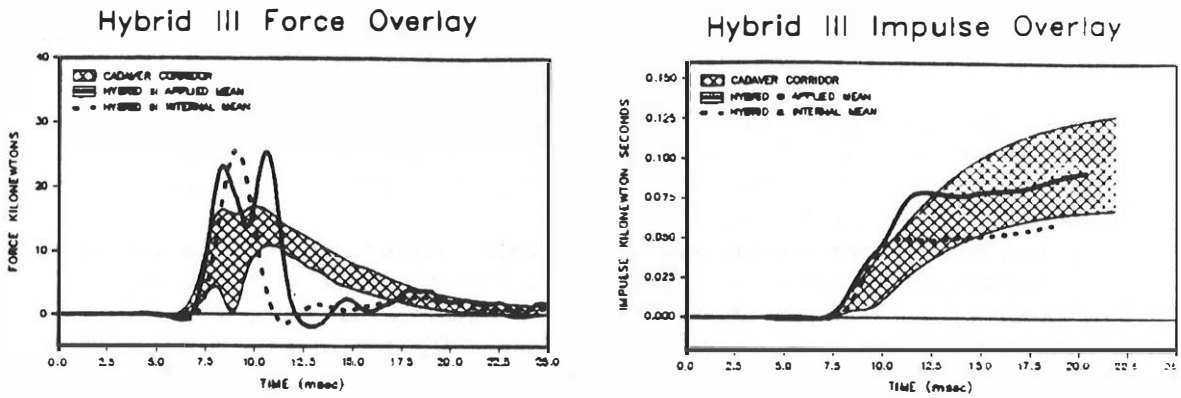

FIG. 17 - CIRA 24 KPH APPLIED FEMUR FORCE AND IMPULSE CORRIDORS

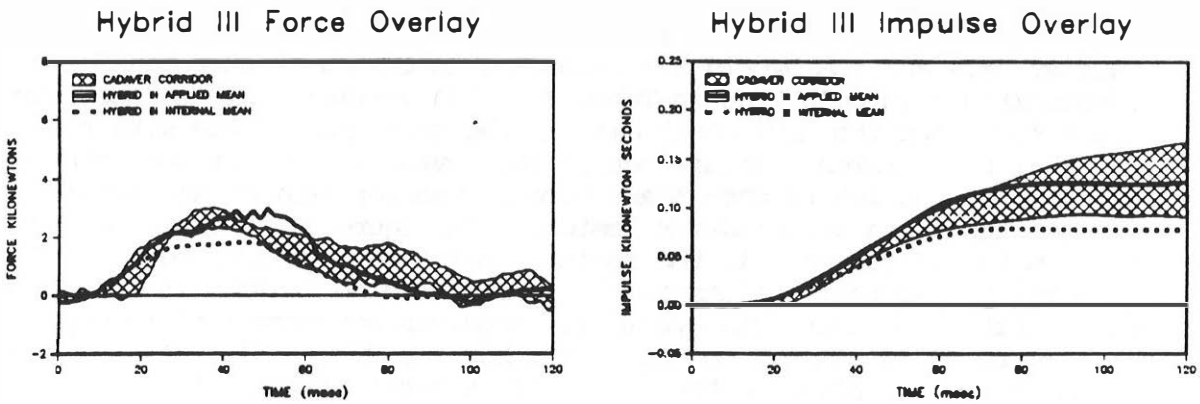

FIG. 18 - CIRA 40 KPH APPLIED FEMUR FORCE AND IMPULSE CORRIDORS

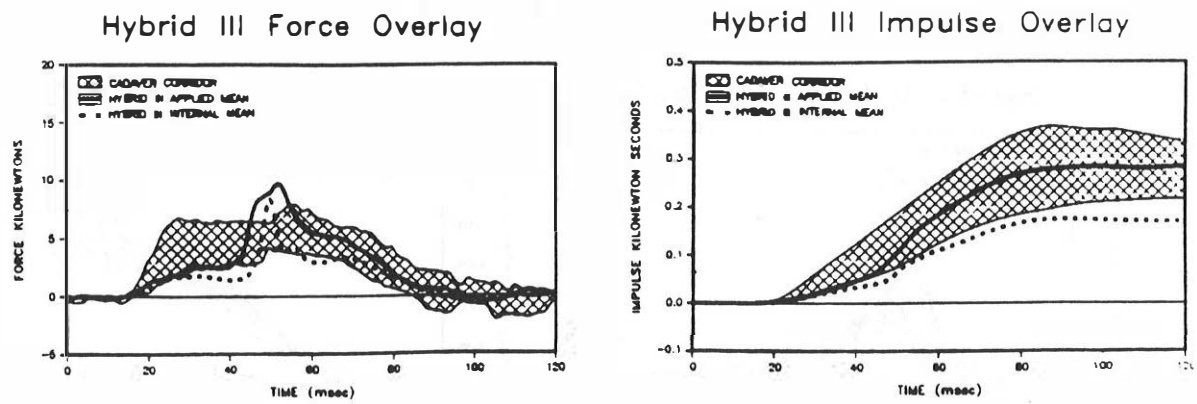

FIG. 19 - WSU 48 KPH SLED EQUIPPED WITH AIR BAG

Hybrid III Applied Force Overlay

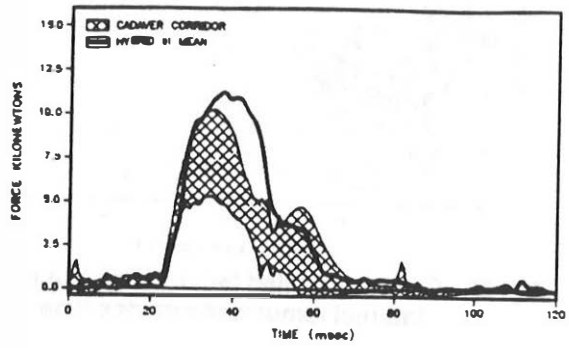

Hybrid III Applied Impulse Overlay

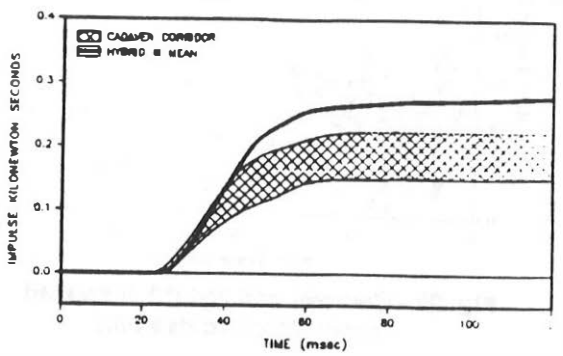

FIG. 20 - WSU 48 KPH (22G) APPLIED FEMUR FORCE AND IMPULSE CORRIDORS

Hybrid III Force Overlay

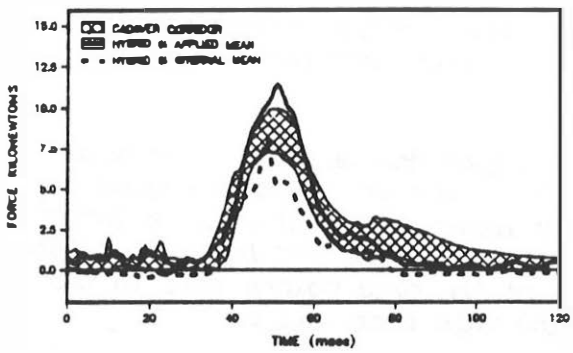

Hybrid III Impulse Overlay

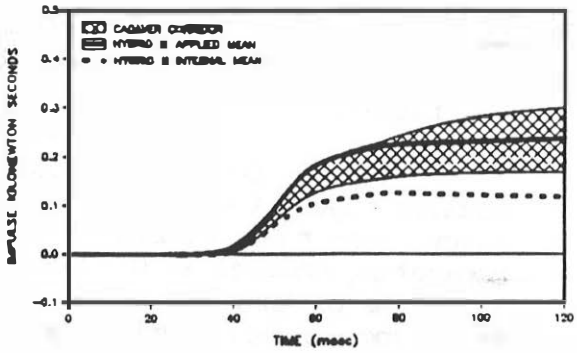

FIG. 21 - WSU 48 KPH (35G) APPLIED FEMUR FORCE AND IMPULSE CORRIDORS

Hybrid III Force Overlay

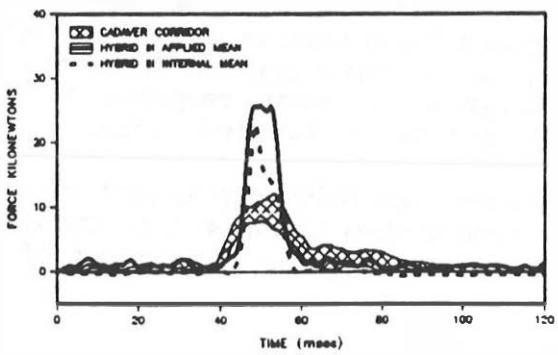

Hybrid III Impulse Overlay

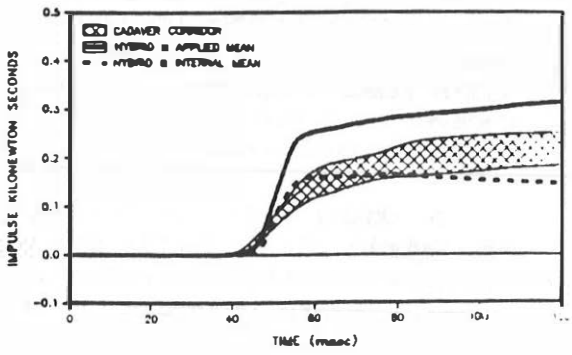

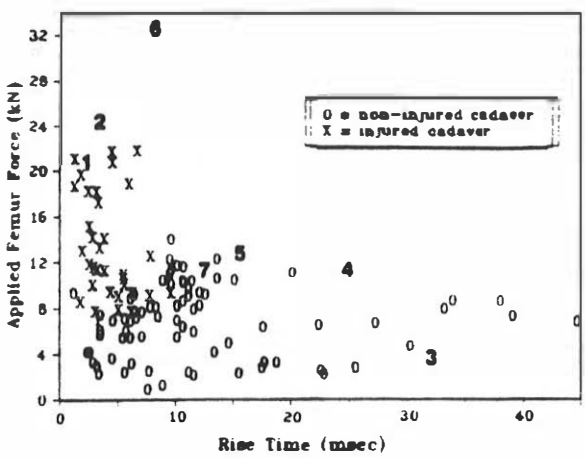

Fig. 22 - Cadaver and Hybrid III applied femur force vs rise time

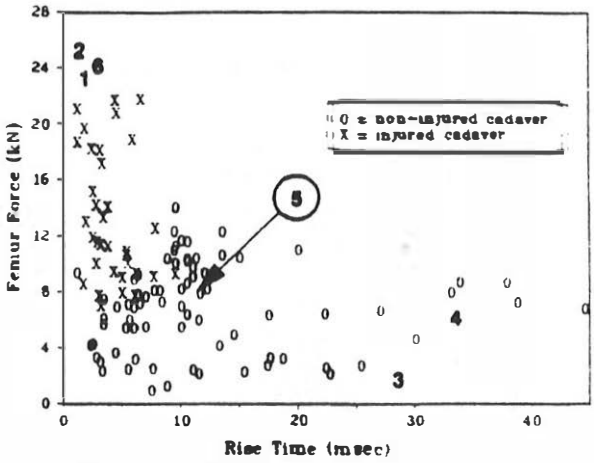

Fig. 23 - Cadaver applied femur force and Hybrid III internal femur force vs rise time

CONCLUSIONS

o In the 1982-1986 NASS files, knee-thigh-hip injuries account for about 12 percent of the total AIS >= 2 lesions for belted drivers and right front seat passengers in frontal collisions. Considering only knee-thigh-hip injuries, fractures account for the major portion of the AIS >= 2 lesions for belted drivers and front seat passengers in frontal collisions.

o Applied femur force alone did a good job of separating human cadaver injury from non-injury although there was a large region of injury/non-injury overlap. An injury index which did an able job of separating cadaver injury/non-injury used the applied femur force and the rise time of that force. About 41 % of the data points fell in the injury/non-injury overlap region using this formulation.

o The femurs of belt or air bag restrained Hybrid IIIs fall in the non-injury region of the previous conclusion. The few femurs which fell in the injury region were associated with higher speed collisions in which intrusion of the firewall and instrument panel occurs.

o The femurs of human cadavers and Hybrid III dummies were identically impact tested in seven separate laboratory test setups. When femur-force-versus-time cadaver corridors and femur-impulse-versus-time cadaver corridors were constructed, comparisons were made with the Hybrid III's femur response. The Hybrid III had a higher applied force than the cadavers for the pendulum tests. The Hybrid III femur response was close to the cadaver corridors for four out of five of the sled tests.

o Using either of the aforementioned knee-thigh-hip injury indices, the Hybrid III correctly predicts no injury when there were no cadaverous lesions and injury when there were cadaverous lesions for six out of the seven separate laboratory conditions.

TABLE 1 - HYBRID III VEHICLE TESTS

Test No.	Closing Speed (kph)	Restraint Used	Vehicle Make	Vehicle Model	Vehicle Year	Internal Femur Force (kN)	Internal Femur Duration (msec)	Internal Femur Rise Time (msec)
CAR TO CAR								
1PL	100	N	Dodge	Omni	83	8.7	50	16
2PL	101	N	Renault	Fuego	83	16.7	40	17
2PR	101	N	Renault	Fuego	83	13.4	34	5
3PR	101	N	Honda	Accord	83	15.2	31	14
3PL	101	N	Honda	Accord	83	12.3	76	48
4PR	100	N	Chevrolet	Celebrity	83	7.4	52	17
4PL	100	N	Chevrolet	Celebrity	83	9.6	53	29
5DL	97	N	Honda	Accord	84	4.6	62	41
5DR	97	N	Honda	Accord	84	9.1	48	19
5PL	97	N	Honda	Accord	84	7.2	72	50
5PR	97	N	Honda	Accord	84	7.4	61	30
6DL	97	N	Dodge	Omni	83	4.5	54	3
6DR	97	N	Dodge	Omni	83	5.7	56	7
6PL	97	N	Dodge	Omni	83	4.7	59	26
6PR	97	N	Dodge	Omni	83	8.7	53	33
7DL	97	N	Renault	Fuego	83	11.4	62	20
7DR	97	N	Renault	Fuego	83	6.1	56	12
7PL	97	N	Renault	Fuego	83	9.5	48	14
7PR	97	N	Renault	Fuego	83	11.9	43	13
8DL	97	N	Honda	Accord	84	6.2	67	26
8DR	97	N	Honda	Accord	84	4.3	46	8
8PL	97	N	Honda	Accord	84	8.9	71	41
8PR	97	N	Honda	Accord	84	6.6	54	37
8DL	97	N	Renault	Fuego	82	7.2	58	23
8DR	97	N	Renault	Fuego	82	4.4	64	24
8PL	97	N	Renault	Fuego	82	10.2	44	17
8PR	97	N	Renault	Fuego	82	9.6	58	16
9DL	89	3M	Honda	Accord	84	2.6	59	6
9DR	89	3M	Honda	Accord	84	2.4	18	6
9PL	89	N	Honda	Accord	84	10.2	61	42
9PR	89	N	Honda	Accord	84	7.8	51	32
9DL	89	N	Chevrolet	Celebrity	84	3.5	89	40
9DR	89	N	Chevrolet	Celebrity	84	2.1	58	24
9PR	89	3M	Chevrolet	Celebrity	84	1.1	21	11
10DL	88	3M	Honda	Accord	84	2.5	44	18
10PL	88	N	Honda	Accord	84	12.0	54	33
10PR	88	N	Honda	Accord	84	10.2	31	7
10DL	88	N	American	Concord	82	5.8	41	5
10DR	88	N	American	Concord	82	7.8	24	5
10PL	88	3M	American	Concord	82	1.5	40	17
10PR	88	3M	American	Concord	82	1.4	46	17
11DL	89	3M	Dodge	Omni	83	3.0	17	5
11DR	89	3M	Dodge	Omni	83	2.9	17	10
11PL	89	N	Dodge	Omni	83	5.9	58	22
11PR	89	N	Dodge	Omni	83	6.9	52	16
11DL	89	N	American	Concord	82	5.1	33	7
11DR	89	N	American	Concord	82	7.0	40	6
11PL	89	3M	American	Concord	82	1.4	40	22
12DR	91	3M	Renault	Fuego	83	2.1	23	12
12PL	91	N	Renault	Fuego	83	12.0	49	18
12PR	91	N	Renault	Fuego	83	8.3	42	15
12DL	91	N	Chevrolet	Celebrity	83	8.4	49	12
12DR	91	N	Chevrolet	Celebrity	83	5.4	62	17
13DR	96	3M	Dodge	Omni	83	9.8	16	5
13DL	96	3M	Dodge	Omni	83	3.3	96	22
13PL	96	3M	Dodge	Omni	83	1.9	17	8
13PR	96	3M	Dodge	Omni	83	1.4	58	20
13DL	96	N	Dodge	Omni	83	7.8	75	16
13DR	96	N	Dodge	Omni	83	7.0	21	9
14DL	95	3M	Honda	Accord	84	6.5	88	34
14DR	95	3M	Honda	Accord	84	2.9	10	4
14PL	95	N	Honda	Accord	84	10.0	81	36
14DR	95	N	Honda	Accord	84	3.8	48	17
14PL	95	3M	Honda	Accord	84	1.8	27	2
14PR	95	3M	Honda	Accord	84	1.3	52	12
15DL	95	N	Renault	Fuego	83	6.8	108	61
15DR	95	N	Renault	Fuego	83	7.7	27	12
16PL	94	N	Honda	Accord	84	3.8	83	35
16PR	94	N	Honda	Accord	84	1.7	22	18
16DL	94	3M	Honda	Accord	84	5.8	137	28
16DR	94	3M	Honda	Accord	84	5.3	37	20
16DR	94	3M	Renault	Fuego	83	3.8	28	13
16PL	94	N	Renault	Fuego	83	6.9	65	39
16PR	94	N	Renault	Fuego	83	2.3	54	26
17DL	87	3M	Chevrolet	Celebrity	83	1.6	98	6
17DR	87	3M	Chevrolet	Celebrity	83	2.9	23	13
18DL	96	N	Dodge	Omni	83	4.1	65	46
18DR	96	N	Dodge	Omni	83	4.2	34	6
18PL	96	N	Dodge	Omni	83	4.5	28	12
18PR	96	N	Dodge	Omni	83	6.1	55	27
19DL	81	N	Chevrolet	Cavalier	84	3.3	91	30
19DR	81	N	Chevrolet	Cavalier	84	4.3	86	23
19DL	81	N	Chevrolet	Cavalier	84	1.8	67	29
19DR	81	N	Chevrolet	Cavalier	84	4.8	56	30
19PL	81	N	Chevrolet	Cavalier	84	4.8	64	13
19PR	81	N	Chevrolet	Cavalier	84	8.8	62	16
19PL	81	N	Chevrolet	Cavalier	84	4.8	74	38
19PR	81	N	Chevrolet	Cavalier	84	5.8	85	22
20DL	82	N	Chevrolet	Cavalier	84	4.7	92	24
20DR	82	N	Chevrolet	Cavalier	84	4.5	72	16
20PL	82	N	Chevrolet	Cavalier	84	5.8	66	20
20PR	82	N	Chevrolet	Cavalier	84	6.9	69	38
20DL	82	N	Chevrolet	Cavalier	84	3.7	82	28
20DR	82	N	Chevrolet	Cavalier	84	6.5	42	20
20PL	82	N	Chevrolet	Cavalier	84	5.6	59	5
20PR	82	N	Chevrolet	Cavalier	84	8.8	68	20

Test Number Codes:

P = passenger
D = Driver
L = left femur
R = right femur

Restraint Codes:

N = None
2M = 2-pt manual belt
3M = 3-pt manual belt
2A = 2-pt automatic belt
2AL = 2-pt automatic belt w/lap belt
3A = 3-pt automatic belt
AB = air bag with lap belt

All forces processed with an SAE Class 180 filter.

(Continued)

TABLE 1 - HYBRID III VEHICLE TESTS (continued)

Test No.	Closing Speed (kph)	Restraint Used	Vehicle Make	Vehicle Model	Vehicle Year	Internal Femur Force (kN)	Internal Femur Duration (msec)	Internal Femur Rise Time (msec)
CAR TO CAR								
21DL	57	3H	Toyota	Celica	89	3.7	55	3
21DR	57	3H	Toyota	Celica	89	4.5	25	2
21PL	57	3H	Toyota	Celica	89	1.3	31	3
21PR	57	3H	Toyota	Celica	89	1.0	21	11
22DL	112	3H	Toyota	Celica	89	1.5	11	3
22DR	112	3H	Toyota	Celica	89	3.2	20	5
22PL	112	3H	Toyota	Celica	89	1.8	18	11
22PR	112	3H	Toyota	Celica	89	1.7	10	2
23DL	110	2AL	Hyundai	Excel	89	10.9	21	13
23DR	110	2AL	Hyundai	Excel	89	11.4	32	12
23PL	110	2AL	Hyundai	Excel	89	7.6	44	3
23PR	110	2AL	Hyundai	Excel	89	4.2	38	7
24DL	114	2AL	Hyundai	Excel GLS	89	9.5	46	13
24DR	114	2AL	Hyundai	Excel GLS	89	13.8	22	13
24PL	114	2AL	Hyundai	Excel GLS	89	8.0	57	4
24PR	114	2AL	Hyundai	Excel GLS	89	5.3	37	13
CAR TO BARRIER								
25DL	48	N	Chevrolet	Celebrity	83	5.5	85	24
25DR	48	N	Chevrolet	Celebrity	83	5.0	40	7
26PL	48	N	Chevrolet	Celebrity	83	0.7	96	36
27DL	48	N	Pontiac	Fiero	84	4.9	57	40
27DR	48	N	Pontiac	Fiero	84	5.2	47	33
28PL	48	N	Pontiac	Fiero	84	6.7	57	37
28PR	48	N	Pontiac	Fiero	84	10.2	62	48
29DL	48	3H	Honda	Accord	84	4.7	55	14
29DR	48	3H	Honda	Accord	84	3.8	36	12
30DL	48	3H	Dodge	Omni	83	4.1	25	9
30DR	48	3H	Dodge	Omni	83	3.1	18	4
30PL	48	N	Dodge	Omni	83	8.4	77	40
30PR	48	N	Dodge	Omni	83	4.5	48	25
31PL	48	N	Renault	Fuego	83	7.7	51	18
31PR	48	N	Renault	Fuego	83	8.3	55	17
32DL	48	2A	VW	Rabbit	84	5.4	59	25
32DR	48	2A	VW	Rabbit	84	4.7	55	21
32PL	48	2A	VW	Rabbit	84	7.7	58	18
32PR	48	2A	VW	Rabbit	84	5.3	54	21
33DL	48	2A	VW	Rabbit	82	6.5	45	19
33DR	48	2A	VW	Rabbit	82	6.3	45	19
33PL	48	2A	VW	Rabbit	82	7.5	57	25
33PR	48	2A	VW	Rabbit	82	5.5	56	14
34DL	48	3H	Honda	Accord	84	4.4	80	46
35DL	48	3H	Dodge	Omni	83	2.1	26	11
35DR	48	3H	Dodge	Omni	83	1.2	49	14
36DL	48	2H	VW	Golf	86	4.0	138	22
36DR	48	2H	VW	Golf	86	7.1	33	14
37DL	41	N	Chevrolet	Cavalier	84	4.8	68	24
37DR	41	N	Chevrolet	Cavalier	84	4.7	53	28
37PL	41	N	Chevrolet	Cavalier	84	5.0	61	37
38DL	47	2A	Chrysler	Le Baron	87	3.7	48	16
CAR TO BARRIER								
38DR	47	2A	Chrysler	Le Baron	87	6.4	61	21
38PL	47	2A	Chrysler	Le Baron	87	3.9	71	16
38PR	47	2A	Chrysler	Le Baron	87	3.9	66	22
39DL	47	2A	Subaru	XT	87	3.5	76	44
39DR	47	2A	Subaru	XT	87	4.8	49	34
39PL	47	2A	Subaru	XT	87	2.3	75	10
39PR	47	2A	Subaru	XT	87	2.1	97	46
40DR	40	N	Hyundai	Excel GLS	87	4.2	61	5
40DL	40	N	Hyundai	Excel GLS	87	6.9	71	10
41DR	40	N	Toyota	Celica	87	6.3	50	7
41DL	40	N	Toyota	Celica	87	4.6	56	23
42DR	57	N	Toyota	Celica	87	6.2	53	14
42DL	57	N	Toyota	Celica	87	10.2	46	16
43DR	56	N	Hyundai	Excel GLS	87	6.2	55	28
43DL	56	N	Hyundai	Excel GLS	87	11.4	51	9
44DL	48	2A	Toyota	Camry	87	6.7	59	24
44DR	48	2A	Toyota	Camry	87	6.7	48	17
44PL	48	2A	Toyota	Camry	87	5.5	49	20
44PR	48	2A	Toyota	Camry	87	6.1	50	15
45DL	47	2A	Ford	Escort	87	3.8	63	26
45DR	47	2A	Ford	Escort	87	3.5	62	9
45PL	47	2A	Ford	Escort	87	2.8	83	55
45PR	47	2A	Ford	Escort	87	4.2	80	43
46DR	48	N	Toyota	Celica	87	5.8	51	17
46DL	48	N	Toyota	Celica	87	4.1	52	27
47DR	39	N	Hyundai	Excel GLS	87	3.5	41	21
47DL	39	N	Hyundai	Excel GLS	87	6.7	54	14
48DR	56	N	Toyota	Celica	87	5.2	58	17
48DL	56	N	Toyota	Celica	87	6.8	52	24
49DR	56	N	Hyundai	Excel GLS	87	7.1	51	19
49DL	56	N	Hyundai	Excel GLS	87	13.0	45	6
50DL	48	1A	Chevrolet	Corsica	89	2.2	43	11
50DR	48	1A	Chevrolet	Corsica	89	6.2	35	7
50PL	48	1A	Chevrolet	Corsica	89	4.8	47	18
50PR	48	1A	Chevrolet	Corsica	89	4.2	63	23
51DL	48	1A	Pontiac	Grand Prix	89	5.5	47	25
51DR	48	1A	Pontiac	Grand Prix	89	4.7	41	18
51PL	48	1A	Pontiac	Grand Prix	89	2.9	45	34
51PR	48	1A	Pontiac	Grand Prix	89	3.0	52	39
52DL	47	AB	Dodge	Diplomat	89	6.0	71	51
52DR	47	AB	Dodge	Diplomat	89	5.8	69	44
53DL	48	1A	Chevrolet	Lumina	90	3.4	59	16
53DR	48	1A	Chevrolet	Lumina	90	5.4	49	10
53PL	48	1A	Chevrolet	Lumina	90	1.2	29	21
53PR	48	1A	Chevrolet	Lumina	90	2.2	55	27
54DL	48	AB	Dodge	Dynasty	90	4.5	94	61
54DR	48	AB	Dodge	Dynasty	90	5.0	79	52
55DL	48	AB	Dodge	Spirit	90	5.6	50	8
55DR	48	AB	Dodge	Spirit	90	5.6	48	10

Test Number Codes:

P = passenger
D = driver
L = left femur
R = right femur

Restraint Codes:

N = None
2H = 2-pt manual belt
3H = 3-pt manual belt
2A = 2-pt automatic belt
2AL = 2-pt automatic belt w/lap belt
3A = 3-pt automatic belt
AB = air bag with lap belt

All forces processed with an SAE Class 180 filter.

TABLE 2 - HYBRID III PENDULUM AND SLED TESTS

Test Number	Test Type (Plot Symbol)	Internal Femur Force (kN)	Internal Femur Impulse (kN*sec)	Internal Force Duration (msec)	Internal Force Rise Time (msec)	Applied Femur Force (kN)	Applied Femur Impulse (kN*sec)	Applied Force Duration (msec)	Applied Force Rise Time (msec)	Delta V (kph)
	CALSPAN CORPORATION									
C87101D	●	13.3	0.06	4	2	13.1	0.10	5	3	14
C87102D	●	13.0	0.06	4	2	13.1	0.10	5	3	14
C87003D	●	13.0	0.06	4	2	12.7	0.10	5	3	14
C87004D	●	12.8	0.06	4	2	13.1	0.10	5	3	14
C87111D	1	23.3	0.10	4	2	20.8	0.17	5	2	26
C87019D	2	25.3	0.10	3	2	24.4	0.18	5	3	25
C87020D	2	26.0	0.11	3	2	26.6	0.19	5	4	28
	UNIVERSITY OF CALIFORNIA AT SAN DIEGO (CIRA)									
S85013D	▲	2.5	0.14	72	36	4.8	0.18	64	42	34
S85113D	▲	2.5	0.11	70	46	4.5	0.19	72	34	34
S85014D	▲	2.5	0.12	66	40	5.4	0.18	59	32	34
S85114D	▲	2.2	0.11	70	34	5.9	0.19	62	37	34
S85015D	3	1.8	0.07	56	29	3.6	0.14	70	32	26
S85115D	3	2.1	0.10	69	24	3.5	0.14	63	47	26
S85016D	3	2.0	0.08	55	26	2.5	0.11	64	22	24
S85116D	3	1.8	0.08	60	38	3.4	0.12	68	41	24
S85017D	4	8.3	0.21	68	31	10.8	0.31	66	30	43
S85117D	4	6.2	0.15	67	34	11.3	0.25	58	25	43
S85018D	4	11.0	0.20	42	8	14.5	0.31	54	21	40
S85118D	4	4.8	0.15	65	31	9.8	0.25	59	27	40
S85019D	4	9.5	0.18	59	28	10.5	0.27	56	27	40
S85119D	4	11.1	0.16	33	6	15.0	0.27	35	7	40
	WAYNE STATE UNIVERSITY									
W85001D	6	8.1	0.12	24	12	12.8	0.23	29	16	47
W85101D	6	8.3	0.14	39	11	10.5	0.23	40	14	47
W85005D	★	10.5	0.14	19	8	18.1	0.36	22	10	48
W85105D	★	10.8	0.13	17	7	16.2	0.36	22	10	48
W85009D	8	24.2	0.16	12	3	33.5	0.29	15	8	48
W85019D	8	22.1	0.18	12	4	30.4	0.22	11	4	48
W85011D	■	6.6	0.11	26	14	14.4	0.38	33	14	48
W85111D	■	7.1	0.12	30	11	13.9	0.30	30	17	48
A81029D	7	NA	NA	NA	NA	11.4	0.25	33	13	48
A81129D	7	NA	NA	NA	NA	11.3	0.32	38	13	48

All forces processed with an SAE Class 180 filter.

1 Pendulum impact where face is covered with five cm polyurethane foam pad; run at 27 kph. (Ref. 17 & 18)

2 Pendulum impact with flat face; run at 27 kph. (Ref. 17 & 18)

3 Sled with an energy absorbing steering wheel; run at 24 kph. (Ref. 19)

4 Sled with an energy absorbing steering wheel; run at 40 kph. (Ref. 19)

5 Sled with automatic 2 point belt system and a bolster at a 180-degree knee angle; run at 48 kph (22 g). (Ref. 16)

6 Sled with an automatic 2 point belt system and a bolster at a 60-degree knee angle; run at 48 kph but at a higher g-level (35 g). (Ref. 16)

7 Sled equipped with an airbag; run at 48 kph. (Ref. 15)

● Pendulum impact with flat face; run at 14 kph. (Ref. 17 & 18)

▲ Sled with an energy absorbing steering wheel; run at 34 kph. (Ref. 19)

★ Sled with an automatic 2 point belt system and a bolster at a 60-degree knee angle run at 48 kph (22 g). (Ref. 16)

■ Sled with an automatic 2 point belt system and a bolster at a 180-degree knee angle; run at 48 kph (22 g). (Low knee bolster) (Ref. 16)

ACKNOWLEDGMENTS The Hybrid III runs which match the four cadaver test configurations of Reference 16 were provided as a courtesy by Ford Motor Company. The authors thank Dr. Claude Tarriere and the research team associated with Peugeot-Renault Association (France) for proving us copies of the data produced in 16 human cadaver sled tests.

DISCLAIMER The views presented are those of the authors and are not necessarily those of the National Highway Traffic Safety Administration, U. S. Department of Transportation.

REFERENCES

1. Patrick, L. M., Kroell, C. K., and Mertz, H. J., "Forces on the Human Body in Simulated Crashes," Ninth Stapp Car Crash Conference Proceedings, 1965.

2. Patrick, L. M., Mertz, H. J., and Kroell, C. K., "Cadaver Knee Chest and Head Impact Loads," Eleventh Stapp Car Crash Conference Proceedings, October 1967.

3. Cooke, F. W., and Nagel, D. A., "Biomechanical Analysis of Knee Impact," Thirteenth Stapp Car Crash Conference Proceedings, December 1969.

4. Powell, W. R., Advani, S. H., Clark, R. N., Ojala, S. J., and Holt, D. J., "Investigation of Femur Response to Longitudinal Impact," Eighteenth Stapp Car Crash Conference Proceedings, December 1974.

5. Melvin, J. W., Stalnaker, R. L., Alem, N. M., Benson, J. B., and Mohan, D., "Impact Responses and Tolerance of the Lower Extremities," Nineteenth Stapp Car Crash Conference Proceedings, November 1975.

6. Powell, W. R., Ojala, S. J., Advani, S. H., and Martin, R. B., "Cadaver Femur Responses to Longitudinal Impacts," Nineteenth Stapp Car Crash Conference Proceedings, November 1975.

7. Viano, D. C., "Considerations for a Femur Injury Criterion," Twenty-First Stapp Car Crash Conference Proceedings, October 1977.

8. Leung, Y. C., Hue, B., Payon, A., Tarriere, C., Hamon, H., Got, C., Patel, A., and Hureau, J., "Study of 'Knee-Thigh-Hip' Protection Criterion," Twenty-Seventh Stapp Car Crash Conference Proceedings with International Research Committee on Biokinetics of Impacts, October 1983.

9. Levine, R. S., "A Review of the Long-Term Effects of Selected Lower Limb Injuries," SAE Paper No. 860501, Symposium on Biomechanics and Medical Aspects of Lower Limb Injuries, October 1986.

10. The Abbreviated Injury Scale, American Association for Automotive Medicine, Morton Grove, Illinois, 1980 Revision.

11. MacKenzie, E. J., "The Public Health Impact of Lower Extremity Trauma," SAE Paper No. 861932, Symposium on Biomechanics and Medical Aspects of Lower Limb Injuries, October 1986.

12. Marcus, J. H., and Blodgett, R., "Priorities of Automobile Crash Safety Based on Impairment," Eleventh International Technical Conference on Experimental Safety Vehicles, May 1987.

13. Malliaris, A. C., Hitchcock, R., and Hedlund, J., "A Search for Priorities in Crash Protection, SAE Paper No. 820242, February 1982.

14. Malliaris, A. C., Hitchcock, R., and Hansen, M., "Harm Causation and Ranking in Car Crashes," SAE Paper No. 850090, February 1985.

15. Cheng, R., Yang, K. H., Levine, R. S., King, A. I., and Morgan, R., "Injuries to the Cervical Spine Caused by a Distributed Frontal Load to the Chest," Twenty-Sixth Stapp Car Crash Conference Proceedings, October 1982.

16. Cheng, R., Yang, K., Levine, R. S., and King, A. I., "Dynamic Impact Loading of the Femur Under Passive Restrained Condition," Twenty-Eighth Stapp Car Crash Conference Proceedings, November 1984.

17. Roberts, D. P., Donnelly, B. R., and Morgan, R., "Cadaver Response to Axial Impacts of the Femur," Eleventh International Technical Conference on Experimental Safety Vehicles, May 1987.

18. Donnelly, B. R., and Roberts, D. P., "Comparison of Cadaver and Hybrid III Dummy Response to Axial Impacts of the Femur," Thirty-First Stapp Car Crash Conference Proceedings, November 1987.

19. Morgan, R. M., Schneider, D. C., Eppinger, R. H., Nahum, A. M., Marcus, J. H., Awad, J., Dainty, D., and Forrest, S., "Interaction of Human Cadaver and Hybrid III Subjects with a Steering Assembly," Thirty-First Stapp Car Crash Conference Proceedings, November 1987.

20. Melvin, J. W., and Musholtz, G. S., "Tolerance and Response of the Knee-Femur-Pelvis Complex to Axial Impacts: Impact Sled Tests," University of Michigan, Highway Safety Research Institute, Ann Arbor, Report No. UM-HSRI-80-27, 1980.

21. Morgan, R. M., Eppinger, R. H., and Marcus, J. H., "Human Cadaver Patella-Femur-Pelvis Injury due to Dynamic Frontal Impact to the Patella," Twelfth International Technical Conference on Experimental Safety Vehicles, May 1989.

22. Ran, A., Koch, M. and Mellander, H., "Fitting Injury Versus Exposure Data into a Risk Function," International IRCOBI Conference on the Biomechanics of Impacts, September 1984.

23. Koch, M., "Recent Work with a Method for the Fitting of Injury Versus Exposure Data into a Risk Function," International IRCOBI Conference on the Biomechanics of Impacts, September 1988.

24. Hair, J. F., Anderson, R. E., and Tatham, R. L., Multivariate Data Analysis, Second Edition, Macmillan Publishing Company, 1987.

25. Ray, A. A., ed, "SAS User's Guide: Statistics," SAS Institute Inc., Box 8000, Cary, North Carolina, 1982.

26. States, J. D., "Adult Occupant Injuries of the Lower Limb," SAE Paper No. 861927, Symposium on Biomechanics and Medical Aspects of Lower Limb Injuries, October 1986.

27. Whittaker, E. T., A Treatise on the Analytical Dynamics of Particles and Rigid Bodies, Cambridge University Press, 1965, pg. 47.

28. Eppinger, R. H., Marcus, J. M., and Morgan, R. M., "Development of Dummy and Injury Index for NHTSA's Thoracic Side Protection Research Program," SAE Paper No. 840885, May 1984.